5th US Combustion Meeting
Organized by the Western States Section of the Combustion Institute
and Hosted by the University of California at San Diego
March 25-28, 2007.

A Dynamic Model for the Turbulent Burning Velocity for Premixed Combustion LES

E. Knudsen and H. Pitsch

Department of Mechanical Engineering,
Stanford University, Stanford, California 94305, USA

A somewhat limited number of computationally tractable methods of simulating turbulent premixed combustion currently exist. Most of these methods either directly or indirectly require information about how fast flames propagate in turbulent flow fields. In this work a dynamic model for describing turbulent burning velocities in the context of large eddy simulation (LES) is presented. This model uses a surface filtering procedure that is consistent with standard LES filtering, and that additionally only uses information that comes directly from the flame front. As such, it is consistent with level set methods, where arbitrary constraints can be imposed on the level set field variable away from the flame front. Brief results showing model validation in the context of direct numerical simulation (DNS) are presented.

1 Introduction

Turbulent premixed flames are particularly difficult to describe in the context of Large-Eddy Simulation (LES). Most industrially relevant premixed flames exist in either the corrugated flamelets regime or the thin reactions zones regime [1]. The width of the inner reaction zone of a flame in these regimes is comparable to, if not smaller than, the Kolmogorov length scale that describes the size of the smallest turbulent eddies in the flow. Flame preheat zones, which are typically much broader than reaction zones, may also, in the corrugated flamelets regime, exist on sub-Kolmogorov length scales. In LES, by definition, the smallest length scales of a flow are filtered out. As a result, in industrially relevant regimes the transitions that occur between unburned and burned states occur on subfilter scales.

Premixed combustion models for implicitly filtered LES that use standalone progress variable or finite rate chemistry approaches will thus, it seems, always fail. All models are limited by the accuracy of the schemes they use for evaluating gradients, and no scheme is capable of resolving the sharp subgrid transitions that occur in premixed implicit LES near flame fronts. Premixed implicit LES models that attempt to resolve flame structure are therefore especially prone to numerical errors in the most critical regions of the flowfield.

In response to the problem of subfilter transition, level set methods such as the G-equation have been suggested as a means of simulating premixed turbulent combustion [1–3]. In these methods, flame fronts are described using isocontours of field variables. At the relevant isocontours, the field variables are governed by equations describing how the fronts propagate. Away from the relevant isocontours, smooth gradients are prescribed for the field variables to ensure numerical resolution.

In these methods, the inner reaction zones of premixed flames are treated as coherent structures. The effect of the chemical activity that occurs within reaction zones appears in level set equations almost entirely as a front propagation speed. This speed, which is approximately equivalent to the laminar burning velocity in the unfiltered case, is therefore one of the most significant modeling inputs in LES of premixed turbulent combustion. Traditional burning velocity models rely on a series of coefficients that have been determined through analyses of both experimental and direct numerical simulation (DNS) data [3, 4]. These coefficient-based approaches have been successfully applied in the context of RANS, where level set methods offer an alternative to the problem of reaction rate closure [3, 5]. In LES, however, where instantaneous flame realizations are available, it should be possible to eliminate the use of constant coefficients by employing dynamic procedures that determine coefficients automatically.

Im *et al.* [6, 7], for example, proposed a dynamic level set propagation model in which level set field variables are treated as scalars. Subfilter contributions to front propagation are determined by evaluating burning velocities at two different filter levels and comparing the results to differences in the magnitude of the gradient of the level set field variable at those same two levels. Im *et al.* claim that this approach can be physically interpreted as enforcing flame consumption conservation. They base this claim on work by Kerstein *et al.* [8] where it was demonstrated that a volume average of the magnitude of the gradient of the level set field variable is equivalent to a measure of the total front area within the volume. In Kerstein *et al.*'s work, each isocontour of the level set field variable was treated as an equally valid representation of the flame front. Under this assumption, volume averaging is equivalent to averaging over multiple front realizations.

More recent work [2, 3, 9] has stressed that level set governing equations are only valid at the field variable isocontour that they describe, and that traditional averaging procedures therefore cannot be used. Specifically, because the value of a level set field variable can be arbitrarily defined away from an isoconotour describing a flame front, volume averaging procedures can produce arbitrary results. In the present paper, then, a dynamic burning velocity model is proposed that only considers information directly from the 2-D front of interest. This model requires the use of a unique filtering approach that is developed and presented in Section 2. In Section 3, the new filtering technique is applied to develop the dynamic model. Section 4 presents an evaluation of the model in the context of DNS. Brief conclusions are offered in Section 5.

2 A governing equation for a premixed flame front

Level set equations can be derived by setting the substantial derivative of a generic field variable equal to zero at a surface of interest. The resulting expression describes how the field variable isocontour associated with that surface evolves. In premixed LES, the derivation of an equation governing flame front behavior can be approached in a different way. A flame front can generally be defined as an isocontour of a generic progress variable c. This variable might represent, for example, a non-dimensionalized temperature. The equation governing the behavior of such a variable is

$$\frac{\partial c}{\partial t} + u_j \frac{\partial c}{\partial x_j} = \frac{1}{\rho} \frac{\partial}{\partial x_j} \left(\rho D \frac{\partial c}{\partial x_j} \right) + \frac{1}{\rho} \dot{\omega}_R, \tag{1}$$

where u_j is the local flow velocity in the jth direction, ρ is the fluid density, D is the diffusivity of the variable c, and $\dot{\omega}_R$ is a source term that describes the effects of chemical reactions. To derive

an equation describing the flame front associated with a particular c isosurface, information from Eq. (1) needs to be extracted directly from this isosurface, here arbitrarily defined as $c = c_0$. This extraction operation can be performed by multiplying Eq. (1) with a delta function, $\delta(c - c_0)$,

$$\delta(c - c_0)\left[\frac{\partial c}{\partial t} + u_j\frac{\partial c}{\partial x_j}\right] = \delta(c - c_0)\left[\frac{1}{\rho}\frac{\partial}{\partial x_j}\left(\rho D\frac{\partial c}{\partial x_j}\right) + \frac{1}{\rho}\dot{\omega}_R\right]. \tag{2}$$

This delta function does not necessarily need to be an infinitesimally thin Dirac delta. Rather, here δ will be defined as a normalized Gaussian of finite width. As long as this width is small compared with the length scale associated with the inner reaction zone of a flame, multiplication with $\delta(c - c_0)$ will effectively give a null result everywhere except at the flame front. This finite width definition of δ is convenient because it eliminates the problem of dealing with the special mathematical properties of the Dirac delta.

Just as Dirac delta functions may equivalently be written as derivatives of heaviside functions, Gaussians may equivalently be written as derivatives of error functions. Since the δ function that appears in Eq. (2) only depends on c, the chain rule may be used to rewrite the left-hand side of Eq. (2). Remembering that what here will be referred to as the heaviside function H represents an error function of finite width, this procedure gives

$$\delta(c - c_0)\left[\frac{\partial c}{\partial t} + u_j\frac{\partial c}{\partial x_j}\right] = \frac{\partial\left[H(c - c_0)\right]}{\partial t} + u_j\frac{\partial\left[H(c - c_0)\right]}{\partial x_j}. \tag{3}$$

To move the delta function on the right-hand side of Eq. (2) into the relevant derivatives, the gradient of the progress variable must first be written in terms of the front normal direction at c_0, which here will be denoted n_j,

$$\frac{\partial c}{\partial x_j} = \frac{\nabla c}{|\nabla c|}|\nabla c| = n_j|\nabla c|. \tag{4}$$

Use of the product rule on the diffusive term then gives

$$\frac{\partial}{\partial x_j}\left(\rho D\frac{\partial c}{\partial x_j}\right) = \rho D|\nabla c|\frac{\partial n_j}{\partial x_j} + n_j\frac{\partial}{\partial x_j}\left(\rho D|\nabla c|\right). \tag{5}$$

Finally, the delta function acts on $|\nabla c|$ as

$$\delta(c - c_0)|\nabla c| = |\delta(c - c_0)\nabla c| = |\nabla\left[H(c - c_0)\right]|. \tag{6}$$

Applying the results of these manipulations to the right-hand side of Eq. (2) produces

$$\delta(c - c_0)\left[\frac{1}{\rho}\frac{\partial}{\partial x_j}\left(\rho D\frac{\partial c}{\partial x_j}\right) + \frac{1}{\rho}\dot{\omega}_R\right] \quad = \tag{7}$$

$$D\kappa|\nabla\left[H(c - c_0)\right]| \quad + \quad \delta(c - c_0)\frac{1}{\rho}\left[n_j\frac{\partial}{\partial x_j}\left(\rho D|\nabla c|\right) + \dot{\omega}_R\right], \tag{8}$$

where κ is the divergence of the normal vector, or the curvature. In summary, then, operating on Eq. (1) with a δ function gives

$$\frac{\partial\left[H(c - c_0)\right]}{\partial t} + u_j\frac{\partial\left[H(c - c_0)\right]}{\partial x_j} \quad = \tag{9}$$

$$D\kappa|\nabla\left[H(c - c_0)\right]| \quad + \quad \delta(c - c_0)\frac{1}{\rho}\left[n_j\frac{\partial}{\partial x_j}\left(\rho D|\nabla c|\right) + \dot{\omega}_R\right]. \tag{10}$$

Equation (10) governs the behavior of a heaviside function that tracks the flame front.

A new variable will now be introduced for the purposes of notational convenience. The variable $\mathcal{G}$ will be defined as

$$\mathcal{G} = H\left(c - c_0\right). \tag{11}$$

A universally valid substitution of $\mathcal{G}$ into Eq. (10) gives

$$\frac{\partial \mathcal{G}}{\partial t} + u_j \frac{\partial \mathcal{G}}{\partial x_j} = D\kappa|\nabla \mathcal{G}| + s_{L,c_0}|\nabla \mathcal{G}|, \tag{12}$$

where

$$s_{L,c_0} = \frac{1}{|\nabla c|\,\rho}\left[n_j \frac{\partial}{\partial x_j}\left(\rho D\,|\nabla c|\right) + \dot{\omega}_R\right]. \tag{13}$$

The quantity s_{L,c_0} describes the propagation velocity of the isosurface $c = c_0$, which is a function of the diffusion and source terms in the progress variable equation, as expected. In the absence of curvature and strain effects, s_{L,c_0} reduces to the unstretched 1-D laminar flame speed s_L. In turbulent settings, however, these effects exist and are important. Although they cause s_{L,c_0} to deviate from s_L, it has been shown that in the absence of high intensity turbulence s_L can reasonably approximate s_{L,c_0} [10].

A further modification to this working definition of propagation speed will be made for convenience. Laminar burning velocities are often provided conditioned on an unburned reference state. To allow such values to be used in the context of the model that will be developed, the same will be done here. The net result of using a 1-D approximation and conditioning, then, is

$$s_{L,c_0} \approx s_L \approx \frac{\rho_u}{\rho} s_{L,u}. \tag{14}$$

Unlike level set variables, $\mathcal{G}$ can be volumetrically filtered because there is nothing arbitrary about its definition. Defining $\mathcal{F}\left(\mathbf{r}\right)$ to be some appropriately normalized filter kernel and then applying it to the $\mathcal{G}$ field gives

$$\overline{\mathcal{G}}\left(\mathbf{x}, t\right) = \int_{|\mathbf{r}|\leq\Delta} \mathcal{F}\left(\mathbf{r}\right)\mathcal{G}\left(\mathbf{x}-\mathbf{r}, t\right) d\mathbf{r} = \int_{|\mathbf{r}|\leq\Delta} \mathcal{F}\left(\mathbf{r}\right) H\left(c\left(\mathbf{x}-\mathbf{r}, t\right) - c_0\right) d\mathbf{r}, \tag{15}$$

where Δ is some characteristic filter width. This filtering procedure is consistent with LES in the sense that the same filter kernel $\mathcal{F}\left(\mathbf{r}\right)$ that is used to filter the Navier-Stokes equations can be used to filter a representation of the flame front. It will be assumed here that the filter kernel $\mathcal{F}\left(\mathbf{r}\right)$ does not change from point to point in physical space $\mathbf{x}$.

This same filter may be applied to Eq. (12). Doing so produces

$$\frac{\partial \overline{\mathcal{G}}}{\partial t} + \overline{u}_j \frac{\partial \overline{\mathcal{G}}}{\partial x_j} + \overline{\Gamma} = D\overline{\kappa\,|\nabla \mathcal{G}|} + \frac{\rho_u}{\overline{\rho}}\overline{s}_T\left|\nabla \overline{\mathcal{G}}\right|, \tag{16}$$

where

$$\overline{\Gamma} = \left(\overline{u_j \frac{\partial \mathcal{G}}{\partial x_j}} - \overline{u}_j \frac{\partial \overline{\mathcal{G}}}{\partial x_j}\right) \tag{17}$$

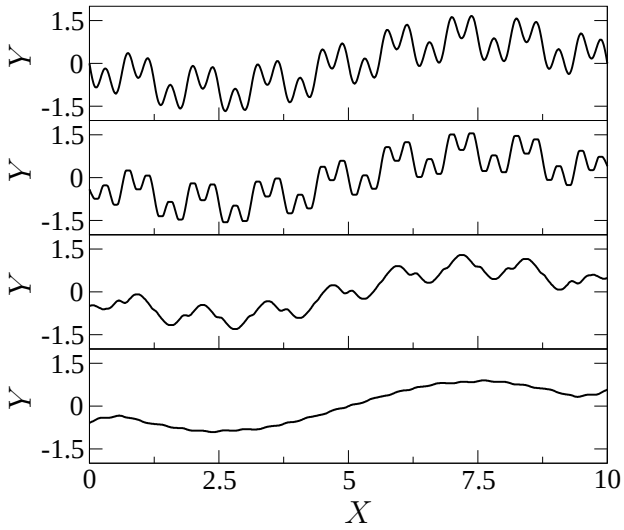

Figure 1: Application of Eq. (15) to the surface $c_0 = 0$ defined by the field variable $c(X,Y) = 1.8\sin\left(\frac{2\pi X}{10}\right) + \sin\left(\frac{16\pi X}{10}\right) + \sin\left(\frac{48\pi X}{10}\right) + 2Y$. The uppermost plot shows the exact surface. The three lower plots show the effects of filters of various widths on the surface. From top to bottom, single filters of widths 0.16, 0.64, and 1.28, respectively, were used. For this example case, a box filter was used for $\mathcal{F}(r)$.

and

$$\frac{\rho_u}{\overline{\rho}}\overline{s}_T\left|\nabla\overline{\mathcal{G}}\right| = \overline{\frac{\rho_u}{\rho}s_{L,u}|\nabla\mathcal{G}|} \tag{18}$$

have been used. Eq. (18) represents the introduction of a model describing the filtered burning velocity, $\overline{s}_T$.

Since this equation has been developed in the context of variable density flows, it is interesting to note what happens when Favre velocity filtering is used. In such cases, all filtered velocities $\overline{u}_j$ are defined as

$$\overline{u}_j(\mathbf{x},t) = \frac{1}{\overline{\rho}(\mathbf{x},t)}\int_{|\mathbf{r}|\leq\Delta}\mathcal{F}(\mathbf{r})\,\rho(\mathbf{x}-\mathbf{r},t)\,u_j(\mathbf{x}-\mathbf{r},t)\,d\mathbf{r}, \tag{19}$$

which leads to the following definition of fluctuating velocities

$$u_j'(\mathbf{x},\mathbf{r},t) = u_j(\mathbf{x}-\mathbf{r},t) - \frac{1}{\overline{\rho}(\mathbf{x},t)}\int_{|\mathbf{r}|\leq\Delta}\mathcal{F}(\mathbf{r})\,\rho(\mathbf{x}-\mathbf{r},t)\,u_j(\mathbf{x}-\mathbf{r},t)\,d\mathbf{r}. \tag{20}$$

When these velocity fluctuations are multiplied with spatial derivatives of $\mathcal{G} = H(c-c_0)$ in the $\overline{\Gamma}$ term, for example, information is retained only directly at the front. The $\overline{\rho}(\mathbf{x},t)$ term in Eq. (20) is therefore simply the front conditioned density, $\overline{\rho}(\mathbf{x},t) = \overline{\rho}(c_0)$. In this sense, all fluctuating velocities in Eq. (16) are conditioned on the density at the front.

Figure 1 demonstrates how the filtering operation proposed in Eq. (15) affects a 2-D front consisting of a variety of wavenumbers. As shown, a small filter removes only the highest wavenumbers, while larger filters remove smaller and smaller wavenumbers.

Equation (12) is very useful because it is filterable. Even after the application of a filter, however, the equation describes a jump that occurs over a single filter width. It is therefore not numerically

tractable. To numerically solve this equation, a level set technique must be used. The great advantage of deriving Eq. (12) and subsequently Eq. (16) is that the explicit subfilter terms that need to be used in the level set representation are now known.

3 Dynamic propagation model

The existence of the appropriate filtering procedure for flame surfaces developed in the previous section makes it is possible to derive a dynamic identity that describes the speed at which a turbulent front propagates. This identity will be derived using Eq. (12). In some respects, it may be regarded as an analog of Germano's identity.

When a broad test filter, which here will be denoted by the hat operator, is applied to Eq. (16), that equation becomes

$$\widehat{\frac{\partial \overline{\mathcal{G}}}{\partial t}} + \widehat{\overline{u}_j \frac{\partial \overline{\mathcal{G}}}{\partial x_j}} + \widehat{\left(\overline{\Gamma}\right)} = \widehat{\left(D\kappa \left|\nabla \mathcal{G}\right|\right)} + \widehat{\frac{\rho_u}{\overline{\rho}} \overline{s}_T \left|\nabla \overline{\mathcal{G}}\right|}. \tag{21}$$

When the bar and hat filters are instead applied to Eq. (12) in a single operation, a different result is obtained,

$$\frac{\partial \widehat{\overline{\mathcal{G}}}}{\partial t} + \widehat{\overline{u}}_j \frac{\partial \widehat{\overline{\mathcal{G}}}}{\partial x_j} + \widehat{\overline{\Gamma}} = D\kappa \widehat{\left|\nabla \mathcal{G}\right|} + \frac{\rho_u}{\overline{\rho}} \widehat{\overline{s}}_T \left|\nabla \widehat{\overline{\mathcal{G}}}\right|. \tag{22}$$

Equations (21) and (22) form the basis for the development of the dynamic model.

Unlike the subfilter Reynolds stress terms that appear in the filtered Navier-Stokes equations, the subfilter term $\overline{\Gamma}$ is relatively insignificant. Specifically, this term describes how high wavenumber velocity components move the filtered front. They tend to wrinkle the instantaneous front, but they act only along a 2-D surface within the filter volume. When these terms are filtered, therefore, they will on average have no effect on the mean front position. Some of the subfilter velocity fluctuations will tend to move the subfilter front location forward, and some will tend to move the front location backward. But because these fluctuations are all deviations from the local filtered velocity, when integrated along the front over the filter volume, they will all tend to cancel out. To illustrate this point, if a non-propagating front were released in a flowfield of homogeneous isotropic turbulence, subfilter scale velocity fluctuations would exist. But the mean front position would remain stationary, even though the exact front becomes more and more wrinkled. Subfilter velocity fluctuations should therefore be unable to contribute to front propagation on their own. They will contribute to front propagation through the increase in surface area that they promote, but this effect appears through another term in the equation. Therefore, the approximations $\overline{\Gamma} \approx 0$ and $\widehat{\overline{\Gamma}} \approx 0$ will be made.

The broad idea behind deriving a dynamic model for $\overline{s}_T$ is to produce a front speed that ensures mean flame front position is independent of the filter being used. This can be achieved by forcing equations (21) and (22), which were created using different sequences of filter application, to produce equivalent front positions. Since the hat filter in Eq. (21) commutes with derivatives, subtracting these two equations and manipulating produces

$$\widehat{\overline{u}_j \frac{\partial \overline{\mathcal{G}}}{\partial x_j}} - \widehat{\overline{u}}_j \frac{\partial \widehat{\overline{\mathcal{G}}}}{\partial x_j} = \widehat{\left(D\kappa \left|\nabla \mathcal{G}\right|\right)} - D\kappa \widehat{\left|\nabla \mathcal{G}\right|} + \rho_u \left(\widehat{\frac{\overline{s}_T}{\overline{\rho}} \left|\nabla \overline{\mathcal{G}}\right|} - \frac{\widehat{\overline{s}}_T}{\overline{\rho}} \left|\nabla \widehat{\overline{\mathcal{G}}}\right| \right), \tag{23}$$

Again, the terms on the left-hand side describe the effects of filtered velocity fluctuations and so can be dropped.

For the purposes of simplification, the remainder of this paper will consider the corrugated flamelets regime only. This eliminates the need to introduce a model describing the effects of subfilter curvature in Eq. (23). Under this approximation the diffusive terms $D\overline{\kappa\left|\nabla\mathcal{G}\right|}$ and $D\widehat{\kappa\left|\nabla\mathcal{G}\right|}$ can be dropped, and the identity reduces to

$$\frac{\overline{s}_T}{\overline{\rho}}\left|\nabla\overline{\mathcal{G}}\right| = \widehat{\frac{\overline{s}_T}{\overline{\rho}}\left|\nabla\overline{\mathcal{G}}\right|}. \tag{24}$$

LES turbulent burning velocity models usually depend much more strongly on the filtering level at which they act than on space. $\overline{s}_T$ will therefore be drawn outside the filter integral, leaving

$$\frac{\overline{s}_T}{\overline{s}_T} = \frac{\widehat{\overline{\rho}^{-1}\left|\nabla\overline{\mathcal{G}}\right|}}{\overline{\rho}^{-1}\left|\nabla\overline{\mathcal{G}}\right|}. \tag{25}$$

This equation represents the final form of the dynamic identity, but in a practical computation the $\mathcal{G}$ variable will not be available. Again, this is because $\mathcal{G}$ undergoes a sharp transition at the front and is not computationally resolvable. Eq. (25) can be written in a more useful form by manipulating the filter definition. If for the purposes of demonstration the density at the front is assumed to be independent of the filter level, and if the first filter level corresponds to a completely resolved field, then

$$\widehat{\left|\nabla\overline{\mathcal{G}}\right|} = \widehat{\left|\nabla\mathcal{G}\right|} = \int_{r\leq 2\Delta}\mathcal{F}_{2\Delta}\left(\mathbf{r}\right)\left|\nabla H\left(c\left(\mathbf{x}-\mathbf{r},t\right)-c_0\right)\right|d\mathbf{r} \tag{26}$$

$$= \int_{r\leq 2\Delta}\mathcal{F}_{2\Delta}\left(\mathbf{r}\right)\delta\left(c\left(\mathbf{x}-\mathbf{r},t\right)-c_0\right)\left|\nabla c\left(\mathbf{x}-\mathbf{r},t\right)\right|d\mathbf{r}. \tag{27}$$

It will be assumed here that $|\nabla c|$ does not strongly vary along the flame front. This assumption does not exactly hold in a real flame where reaction rates depend to a certain extent on flame curvature [10]. However, it is in agreement with the use of the laminar burning velocity for the description of the reaction and diffusion terms in Eq. (1), and provides leading order accuracy. The benefit of this assumption is that it allows $|\nabla c|$ to be brought out of the integral, which in turn makes it convenient to define a variable describing the amount of front area that exists per filter volume,

$$a_{2\Delta} = \int_{r\leq 2\Delta}\mathcal{F}_{2\Delta}\left(\mathbf{r}\right)\delta\left(c\left(\mathbf{x}-\mathbf{r},t\right)-c_0\right)d\mathbf{r}. \tag{28}$$

When $\mathcal{F}$ is a tophat filter, $a_{2\Delta}$ describes the exact unfiltered flame area within the filter domain. When $\mathcal{F}$ is a Gaussian, $a_{2\Delta}$ gives flame surfaces near the center of the filtering domain more weight. Using these definitions, $\widehat{|\nabla\mathcal{G}|}$ may be rewritten

$$\widehat{\left|\nabla\mathcal{G}\right|} = \left|\nabla c\right|\big|_{c_0}a_{2\Delta}. \tag{29}$$

The denominator of the right hand side of Eq. (25) may be written

$$\left|\nabla\widehat{\overline{\mathcal{G}}}\right| = \left|\nabla c\right|\Big|_{c_0} \left| \int_{r\leq 2\Delta} \mathcal{F}_{2\Delta}\left(\mathbf{r}\right) \delta\left(c\left(\mathbf{x}-\mathbf{r},t\right)-c_0\right) n_j\left(\mathbf{x}-\mathbf{r},t\right) d\mathbf{r} \right| \tag{30}$$

The expression within the absolute value sign approximately describes the area density of the *filtered* flame front within the filter volume. This quantity will be defined as $\widehat{\overline{a}}_{2\Delta}$. Finally, since the right-hand side of Eq. (25) describes flame area densities within the same filter volume, the actual flame areas may be used in the identity,

$$\frac{\overline{s}_T}{\overline{s}_T} = \frac{\overline{A}_{front}}{\widehat{\overline{A}}_{front}}. \tag{31}$$

This form of the identity agrees with Damkohler's hypothesis [11],

$$\frac{s_T}{s_L} \sim \frac{A_{exact}}{A_{mean}}, \tag{32}$$

and enforces the condition that the mass a flame consumes should be independent of filter level.

The remainder of this brief will use a burning velocity model proposed by Peters [2, 3],

$$\frac{s_T - s_L}{u'} = -\gamma \mathrm{Da} + \sqrt{\left(\gamma \mathrm{Da}\right)^2 + \gamma\alpha\mathrm{Da}}. \tag{33}$$

Since it has been assumed for simplicity that in this paper only flames in the corrugated flamelets regime are under consideration, the form that this burning velocity model takes in that regime will be used,

$$s_T = s_L + u'\frac{\alpha}{2}. \tag{34}$$

In what follows, Eq. (31) will be treated as a dynamic identity, Eq. (34) will be used to model s_T, and α in Eq. (34) will be viewed as a dynamic coefficient.

4 DNS Validation

A direct numerical simulation (DNS) of a front propagating in forced homogeneous isotropic turbulence was performed to validate this model. The parameters describing the DNS are shown in Table 1. Turbulence was forced using the linear scheme of Rosales and Meneveau [12], and the simulation was run at a constant density. A uniform cartesian mesh was used, but in the direction of front propagation the domain length was doubled so that front statistics could be gathered for a longer period of time. The level set equation

$$\frac{\partial G}{\partial t} + u_j \frac{\partial G}{\partial x_j} = s_L \left|\nabla G\right| \quad \forall \;\; G = G_0 \tag{35}$$

was solved to describe front evolution. As there are no diffusive terms in this equation, the front effectively resides in the corrugated flamelets regime. A re-initialization procedure was performed after every three time steps to force the level set field variable away from the front to conform to a

Simulation Constants	Turbulence Parameters
Mesh size = 256 x 128 x 128	Re_λ = 39
Δx = $1.0 \cdot 10^{-3}\ m$	Re_t = 101
ν = $1.87 \cdot 10^{-5}\ m^2/s$	Integral length scale, l_t = $7.7 \cdot 10^{-3}\ m$
ρ = $1.16\ kg/m^3$	Eddy turnover time, τ = $0.20\ s$
Burning velocity, $s_L = 0.06\ m/s$	Komogorov scale, η = $5.0 \cdot 10^{-4}\ m$
Forcing coefficient, $A = 2.4$	Largest eddy size, l = $16.0 \cdot 10^{-3}\ m$

Table 1: DNS Parameters

distance function. Reinitialization was accomplished by first using an iterative marker method to estimate the distance to the front, and subsequently solving a PDE in psuedo-time to improve the accuracy of this estimate. The third order WENO scheme of Peng *et al.* [13] was used for the PDE step.

Statistics involving the front itself were computed using information from only one isocontour of the level set field variable. This isocontour was used to compute the area of the flame, as needed in the model. Neumann boundary conditions were prescribed for the level set at each end of the domain in the propagation direction. The front, however, never came so near these boundaries that their treatment influenced behavior. Periodic boundary conditions were prescribed for the level set in the other two directions.

A parallel, structured code that is second order in both time and space was used to compute the flow. Although the code was run using an implicit solver, the CFL number was limited to 0.5 to ensure that all structures were time resolved. Because the linear forcing scheme used here adds energy to the flow at all wavenumbers, the turbulent flowfield was initialized within a 128^3 cube, and then copied to an adjacent cube. This prevented the generation of wavenumbers smaller than the inverse of the box size. Periodic boundary conditions were used in every direction for the velocity field. Figure 2 shows two instantaneous realizations of the flowfield and front.

Figure 3 shows mean front displacement as a function of time, computed both directly from the DNS and from a variety of models. If no turbulent burning velocity model is used, front displacement is severely under-predicted, as expected. The static turbulent burning velocity model of Eq. (34), however, somewhat over-predicts front displacement. This over-prediction primarily develops at early times as the front, which is initially flat, transitions to a wrinkled surface under the influence of turbulence. In contrast, the dynamic model accurately predicts this transition. The solid line, for example, uses unfiltered fields to describe a first filter level, and completely filtered fields to describe a second. Applying Eq. (31) in this context consists of multiplying the laminar burning velocity by the area of the fully resolved front and then dividing the result by the width and height of the domain, which represents the area of the completely filtered front. The results are in excellent agreement with the DNS data.

The dynamic model produces results that are somewhat less accurate when filter levels that are very closely spaced are used. For example, when unfiltered and singly filtered fields are used in Eq. (31), front displacement is mildly over-predicted. This error does not signify a problem with the modeling approach as much as it highlights the difficulty of describing how velocity fluctuations,

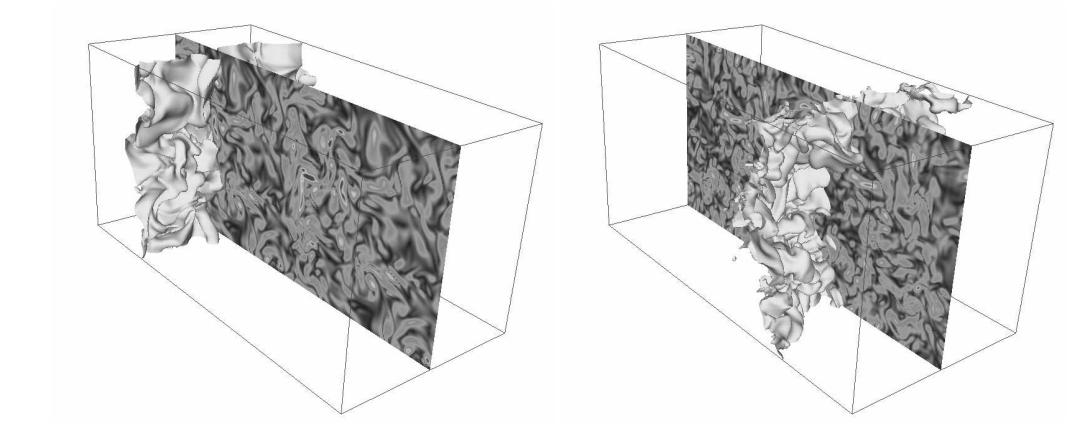

Figure 2: Snapshots from a DNS of front propagation. The level set is the wrinkled surface, and the cut plane shows voriticity magnitude. The left image shows an early time in the simulation, while the right image shows the fully developed front.

u', change with very small changes in filter wavenumber. If the fluctuations are relatively small to begin with, as they are when a singly filtered field is used, all errors made in predicting u' will strongly affect the solution of Eq. (31). The sensitivity of dynamic front propagation models to u' was also noted by Im *et al.* [6] in the context of scalar isosurfaces.

Difficulties in predicting filtered velocity fluctuations are alleviated to a certain extent when the test filters selected span a wider range of wavenumbers. The – · · – line in Fig. 3 shows that dynamic model predictions considerably improve when quadruply filtered and completely filtered fields are used as test levels.

Figure 4 shows speeds and area ratios from both the DNS and the models as a function of time. The front propagation speed that the static turbulent burning velocity model predicts varies smoothly in time, because it depends only on averaged velocity fluctuations that are a function of the amount of kinetic energy in the domain. The actual front propagation velocity, however, oscillates at relatively high frequency. The dynamic model, regardless of the filters used, appropriately captures this high frequency behavior, which appears through the surface area of the front. Specifically, even in the dynamic case that uses unfiltered and singly filtered fields, the area ratio of the fronts that is plotted using the right vertical axis qualitatively matches the plot of the DNS front propagation speed. The errors in the model are therefore due to the scaling of this area ratio, which again is a function of subfilter velocity fluctuations.

Finally, since the model's sensitivity to u' has been emphasized, it is appropriate to describe how this quantity is computed in the DNS. The most critical requirement for this computation is that there be a match between the filtering procedure used on the front area and the procedure used on the velocity field. At a minimum, this means that the filtering kernel $\mathcal{F}$ that is computationally applied to the front should be the same as that applied to the velocity field. Experience showed, however, that this alone was not enough. Attempts to extract differences in u' from turbulent viscosities computed at two filter levels, or from model turbulence spectra mapped onto the velocity fields, proved insufficient. Rather, the energy of the velocity fields at each filter level had to be computed. A difference in the velocity fluctuations associated with different filters could then be

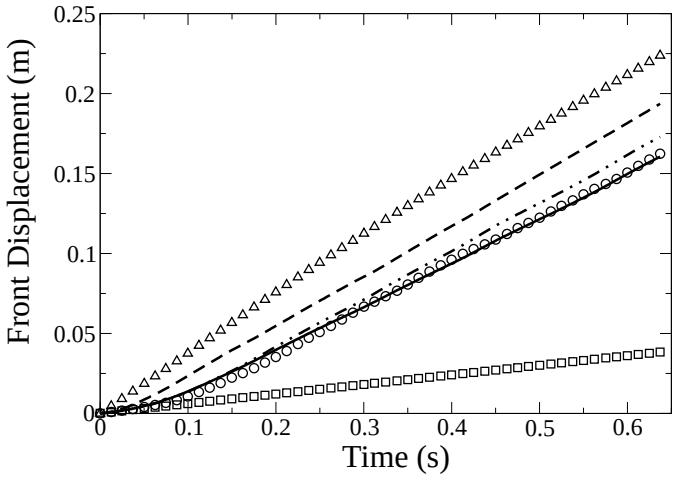

Figure 3: Front displacement from initial location as a function of time, using: ○ : Mean front position from DNS; □ : Laminar burning velocity; △ : Static turbulent burning velocity model (Eq. (34)); ——— : $s_L \frac{A_{unfiltered}}{A_{flat}}$, with area ratio from DNS; – – : Dynamic model computed using unfiltered and singly filtered fields, – · · – : Dynamic model computed using quadruply filtered and completely filtered fields

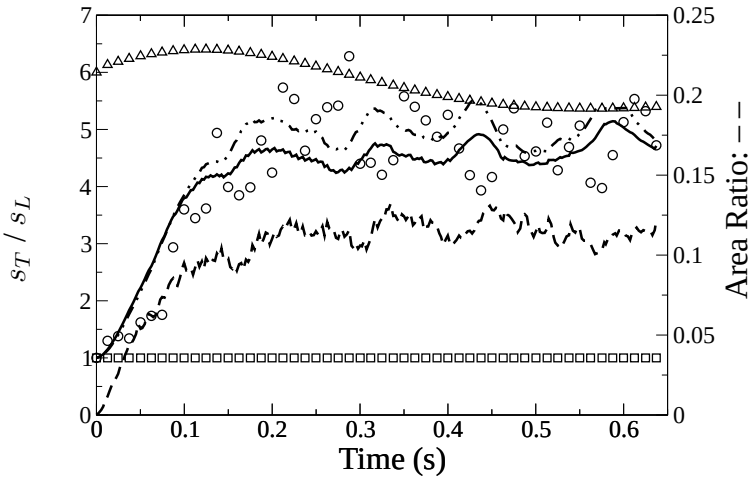

Figure 4: Front speed and area ratio as a function of time: ○ : s_T directly from DNS data; □ : Laminar; △ : Static s_T model (Eq. (34)); ——— : $\frac{s_T}{s_L} = \frac{A_{unfiltered}}{A_{flat}}$, with area ratio from DNS; – – : Area ratio of unfiltered and singly filtered fronts (right vertical axis), – · · – : s_T from dynamic model, computed using quadruply filtered and completely filtered fields

formed,

$$\widehat{\overline{u'}} - \overline{u'} = \sqrt{\frac{2}{3}\overline{k}} - \sqrt{\frac{2}{3}\overline{k}}, \tag{36}$$

where $\overline{k}$ is the kinetic energy associated with the velocity field $\overline{u}_j$. Even when an arbitrary means of computing $\overline{u'}$ was used, this technique accurately described how velocity fluctuations varied with the filter used.

5 Conclusions

In consistent LES procedures, subfilter models should act to ensure that all mean predicted quantities are independent of the filters being used. In this paper, a dynamic model for calculating the propagation speed of flame fronts was presented. This model was derived in a way that ensures that this filter independence criteria is met. In the derivation of this model, a new approach to writing a flame front equation was presented. This approach was useful because it both worked in conjunction with standard LES filtering techniques and because it used information from only a 2-D surface. Using this approach, the terms that describe subfilter influences on the turbulent burning velocity were explicitly determined. Furthermore, these terms were used to derive a dynamic identity for the burning velocity. When enforced, this identity ensures that evolving a flame front and then filtering the result yields the same answer that evolving a filtered front does. In its simplest form, the identity may physically be viewed as an enforcement of flame mass consumption conservation. A DNS was performed to validate the proposed dynamic model. Results showed that the model predicted the speed of a propagating turbulent front with more accuracy than a static turbulent burning velocity model.

Acknowledgements

Support from the United States Department of Defense NDSEG Fellowship Program, and from the United States Air Force Office of Scientific Research (AFOSR), is gratefully acknowledged.

References

[1] H. Pitsch and L. Duchamp De Lageneste. Large-eddy simulation of premixed turbulent combustion using a level set approach. In *Proceedings of the Combustion Institute*, pages 2001–2008. Combustion Institute, 2002.

[2] H. Pitsch. *Combustion and Flame*, 143 (2005) 587–598.

[3] N. Peters. *Turbulent Combustion*. Cambridge University Press, England, 2000.

[4] R. G. Abdel-Gayed and D. Bradley. *Philosophical Transactions of the Royal Society of London A*, 301 (1981) 1–25.

[5] M. Herrmann. *Numerische Simulation vorgemischter und teilweise vorgemischter turbulenter Flammen*. PhD thesis, RWTH Aachen, 2000.

[6] H. G. Im, T. S. Lund, and J. H. Ferziger. *Physics of Fluids*, 9 (1997) 3826–3833.

[7] A. Bourlioux, H. G. Im, and J. H. Ferziger. A dynamic subgrid-scale model for LES of the G-equation. In *Proceedings of the CTR Summer Program*. Stanford University, 1998.

[8] A. R. Kerstein, W. T. Ashurst, and F. A. Williams. *Physical Review A*, 37 (1988) 2728–2731.

[9] M. Oberlack, H. Wenzel, and N. Peters. *Combustion Theory and Modelling*, 5 (2001) 363–383.

[10] T. Echekki and J. H. Chen. *Combustion and Flame*, 118 (1999) 308–311.

[11] G. Damköhler. *Z. Elektrochem.*, 46 (1941) 601–652.

[12] C. Rosales and C. Meneveau. *Physics of Fluids*, 17 (2005) 1–8.

[13] D. Peng, B. Merriman, S. Osher, H. Zhao, and M. Kang. *Journal of Computational Physics*, 155 (1999) 410–438.